Impulsive Electromagnetic Response of Thin Plasmonic Metal Sheets

Martin Štumpf #1 and Guy A. E. Vandenbosch 2

ESAT-TELEMIC, Katholieke Universiteit Leuven
Kasteelpark Arenberg 10, Heverlee (Leuven), Belgium
1 martin.stumpf@esat.kuleuven.be 2 guy.vandenbosch@esat.kuleuven.be

***Abstract*— The impulsive electromagnetic response of a thin metallic coating on a dielectric half-space is analytically investigated. Both TM- and TE-polarized electromagnetic fields in the configuration are excited by an impulsive line source. The problem is solved with the help of approximate thin-film boundary conditions and the Cagniard-DeHoop technique. Closed-form space-time expressions for electromagnetic fields are found, numerically evaluated and discussed with regard to the pulsed excitation of surface plasmon phenomena.**

I. Introduction

The coupling of electromagnetic waves to free electron plasma in metals becomes of great importance to nanophotonics with a wealth of promising applications in sensorics [1], bio-photonics [2], data storage [3] or optical waveguides [4], [5]. A proper understanding of related surface phenomena requires the mathematical analysis of generic configurations where the influence of the system parameters on the performance shows up in closed-form analytic expressions that characterize the physical behavior. The simplest configuration in this context is a planar interface between a metal and a dielectric where the excitation of so-called surface plasmon polaritons is usually demonstrated with the help of a frequency-domain plane-wave solution of macroscopic electromagnetic field equations [6], [7]. Although the pulsed-laser excitation of surface-plasmon resonance is commonly used in a variety of experiments [8], [9], its thorough space-time mathematical description, except for a few initial studies, is missing in the literature. In this respect, Kooij has analyzed the pulsed reflected field above a plasmonic half-space [10] and the time-domain surface impedance of plasmonic half-spaces for plane-wave incidence is investigated in [11].

In this paper the electromagnetic response of a thin plasmonic coating on a dielectric support is found. To this end we apply the concept of approximate thin-sheet boundary conditions [12] together with the Cagniard-DeHoop (CdH) method [13]. The method provides closed-form space-time expressions describing relevant impulsive TE- and TM-polarized electromagnetic fields in the configuration. In them, time evolution of electromagnetic field quantities at different observation positions relative to the source point and their dependence on the metallic film/dielectric support parameters clearly show up. As a consequence, the derived expressions allow us to gain physical insights into the relevant surface/pseudo-surface wave phenomena [14].

On leave from Brno University of Technology, SIX Research Centre, Purkynova 118, 612 00 Brno, the Czech Republic.

II. Problem Formulation

The problem configuration is shown in Fig. 1. In it, the position is localized by the coordinates $\{x_1, x_2, x_3\}$ with respect to a fixed, orthogonal, right-handed Cartesian reference frame. The time coordinate is denoted by t, $*$ denotes the time convolution and ∂_t is the partial differentiation with respect to time.

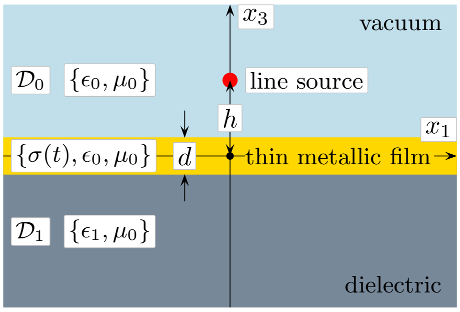

Fig. 1. Problem configuration.

The problem configuration consists of two unbounded domains $\mathcal{D}_0$ and $\mathcal{D}_1$ joined by a metal layer of a vanishing thickness $d \downarrow 0$. Electromagnetic properties of $\mathcal{D}_0$ and $\mathcal{D}_1$ are described by scalar electric permittivity and magnetic permittivity $\{\epsilon_0, \mu_0\}$ and $\{\epsilon_1, \mu_0\}$, respectively. The corresponding electromagnetic wavespeeds are $c_0 = (\epsilon_0\mu_0)^{-1/2} > 0$ and $c_0 > c_1 = (\epsilon_1\mu_0)^{-1/2} > 0$. It is assumed that the metallic layer presents a high contrast in its electric conductivity described by the conduction relaxation function [15, Sec. 19.5]

$$\sigma(t) = \epsilon_0 \omega_P^2 \exp(-\nu_C t)\mathrm{H}(t) \tag{1}$$

where ω_P is the electron plasma angular frequency, ν_C is the collision frequency, ϵ_0 is the electric permittivity of vacuum and $\mathrm{H}(t)$ is the Heaviside unit step function. The metallic sheet supports electric current along $x_3 = 0$ only and its thickness is negligible with respect to the spatial support of the excitation pulse generated by a magnetic line source placed in $\mathcal{D}_0$ at

$(x_1, x_3) = (0, h)$, $h > 0$. On account of the problem configuration, excited electromagnetic fields are x_2-independent. Depending on the nature of the line source, two sets of electromagnetic components can be excited: 1) An electric current line source generates TE fields $\{E_2, H_1, H_3\}$; 2) A magnetic current line source generates TM fields $\{H_2, E_1, E_3\}$. The line sources placed at $(x_1, x_3) = (0, h)$ above the thin sheet are defined via their electric and magnetic current volume densities

$$\{J_2, K_2\}(x_1, x_3, t) = \{i, k\}(t)\delta(x_1)\delta(x_3 - h) \quad (2)$$

respectively. Here, $i(t)\,[\mathrm{A}]$ and $k(t)\,[\mathrm{V}]$ are the source strengths and $\delta(x)$ is the Dirac delta distribution. It is assumed that $\{i, k\}(t) = \{0, 0\}$ for $t < 0$. If the thin metallic film presents a high contrast in electric conductivity, then the approximate thin-sheet boundary conditions are

$$\lim_{x_3 \downarrow 0} \boldsymbol{\nu} \times \boldsymbol{E} - \lim_{x_3 \uparrow 0} \boldsymbol{\nu} \times \boldsymbol{E} = \boldsymbol{0} \quad (3)$$

for all $t \in \mathbb{R}$ and all $x_1 \in \mathbb{R}$ and

$$\lim_{x_3 \downarrow 0} \boldsymbol{\nu} \times \boldsymbol{H} - \lim_{x_3 \uparrow 0} \boldsymbol{\nu} \times \boldsymbol{H} = G_L(t) * \boldsymbol{E}(x_1, 0, t) \quad (4)$$

where $\boldsymbol{\nu}$ is the unit vector in the x_3-direction and the electric conductivity of the sheet is given as

$$G_L(t) = d\sigma(t) \quad (5)$$

The thin-sheet high-contrast boundary conditions require that $d\sigma_0[1 - \exp(-\nu_C t)]$ is of order $O(1)$ as $d \downarrow 0$ which limits the minimal time width of the excitation pulse and σ_0 is the conductivity of stationary currents $\sigma_0 = \epsilon_0 \omega_P^2/\nu_C$ [15, Sec. 19.6]. Note in this respect that the metal film is transparent for extremely short pulses which leads to vanishing scattered fields in the configuration.

III. Transform-domain solution

The Cagniard-DeHoop method combines the unilateral Laplace transformation with the wave slowness field representation. To show the notation, the expressions are given for E_2 field component. The Laplace transformation is defined as

$$\hat{E}_2(x_1, x_3, s) = \int_{t=0}^{\infty} \exp(-st) E_2(x_1, x_3, t)\mathrm{d}t \quad (6)$$

for the real and positive parameter s that is used in the slowness representation applied parallel to the metal sheet

$$\hat{E}_2(x_1, x_3, s) = (s/2\pi\mathrm{i}) \int_{p=-\mathrm{i}\infty}^{\mathrm{i}\infty} \exp(-spx_1) \times \tilde{E}_2(p, x_3, s)\mathrm{d}p \quad (7)$$

The transform-domain solution then follows from the electromagnetic field equations solved together with the boundary conditions (3)–(4) under transformations (6)–(7).

A. TE polarization

The transform-domain solution for TE polarization reads

$$\{\tilde{H}_1, \tilde{H}_3, \tilde{E}_2\} = \{\mp\gamma_0/\mu_0, p/\mu_0, 1\}\tilde{A}_E \exp[-s\gamma_0|x_3 - h|] + \{-\gamma_0/\mu_0, p/\mu_0, 1\}\tilde{A}_E \tilde{R}_E \exp[-s\gamma_0(x_3 + h)] \text{ in } \mathcal{D}_0 \quad (8)$$

$$\{\tilde{H}_1, \tilde{H}_3, \tilde{E}_2\} = \{\gamma_1/\mu_0, p/\mu_0, 1\}\tilde{A}_E \tilde{T}_E \times \exp(-s\gamma_0 h)\exp(s\gamma_1 x_3) \text{ in } \mathcal{D}_1 \quad (9)$$

where $\mp$ applies to $x_3 > h$ and $0 \le x_3 < h$, respectively, and

$$\tilde{R}_E = (\tilde{G}_{E0} - \tilde{G}_{E1} - 2\hat{G}_L)/(\tilde{G}_{E0} + \tilde{G}_{E1} + 2\hat{G}_L) \quad (10)$$

$$\tilde{T}_E = 2\tilde{G}_{E0}/(\tilde{G}_{E0} + \tilde{G}_{E1} + 2\hat{G}_L) \quad (11)$$

$$\tilde{A}_E = -(\mu_0/2\gamma_0)\hat{i}(s) \quad (12)$$

with $\tilde{G}_{E0,1} = 2\gamma_{0,1}/\mu_0$.

B. TM polarization

The transform-domain solution for TM polarization reads

$$\{\tilde{E}_1, \tilde{E}_3, \tilde{H}_2\} = \{\pm\gamma_0/\epsilon_0, -p/\epsilon_0, 1\}\tilde{A}_H \exp[-s\gamma_0|x_3 - h|] + \{\gamma_0/\epsilon_0, -p/\epsilon_0, 1\}\tilde{A}_H \tilde{R}_H \exp[-s\gamma_0(x_3 + h)] \text{ in } \mathcal{D}_0 \quad (13)$$

$$\{\tilde{E}_1, \tilde{E}_3, \tilde{H}_2\} = \{-\gamma_1/\epsilon_1, -p/\epsilon_1, 1\}\tilde{A}_H \tilde{T}_H \times \exp(-s\gamma_0 h)\exp(s\gamma_1 x_3) \text{ in } \mathcal{D}_1 \quad (14)$$

where $\pm$ applies to $x_3 > h$ and $0 \le x_3 < h$, respectively, and

$$\tilde{R}_H = (\tilde{G}_{H1} - \tilde{G}_{H0} + 2\hat{G}_L)/(\tilde{G}_{H1} + \tilde{G}_{H0} + 2\hat{G}_L) \quad (15)$$

$$\tilde{T}_H = 2\tilde{G}_{H1}/(\tilde{G}_{H1} + \tilde{G}_{H0} + 2\hat{G}_L) \quad (16)$$

$$\tilde{A}_H = -(\epsilon_0/2\gamma_0)\hat{k}(s) \quad (17)$$

with $\tilde{G}_{H0,1} = 2\epsilon_{0,1}/\gamma_{0,1}$. In Eqs. (10), (11) and (15), (16), $\hat{G}_L(s) = \beta/(s+\nu_C)$ with $\beta = d\epsilon_0\omega_P^2$. Finally, the propagation coefficients in $\mathcal{D}_{0,1}$ are

$$\gamma_{0,1} = (1/c_{0,1}^2 - p^2)^{1/2} \quad (18)$$

with $\mathrm{Re}(\gamma_{0,1}) > 0$ for all $p \in \mathbb{C}$. Obviously, the first terms in Eqs. (8) and (13) represent the incident wave and the second ones, the reflected waves in $\mathcal{D}_0$. Eqs. (9) and (14) then give the transform-domain expressions for the fields transmitted to the dielectric half-space $\mathcal{D}_1$.

IV. Space-time solution

The solution is found using the Cagniard-DeHoop technique [13]. For the sake of conciseness, final results are provided.

A. TE polarization

The space-time expressions for the TE-polarized fields read the following form

$$\begin{aligned}\{H_1, H_3, E_2\} &= -\partial_t i(t) * \left\{-\frac{(x_3 - h)t}{D_I^2}, \frac{x_1 t}{D_I^2}, \mu_0\right\} \\ &\times (1/2\pi)(t^2 - T_I^2)^{-1/2}\mathrm{H}(t - T_I) \\ &- \partial_t i(t) * \mathrm{Re}\Big[\{-\gamma_0[p(t)], p(t), \mu_0\}\tilde{R}_{E0}[p(t)]\Big] \\ &\times (1/2\pi)(t^2 - T_R^2)^{-1/2}\mathrm{H}(t - T_R) \\ &+ \partial_t i(t) * \frac{1}{2\pi}\int_{\tau=T_R}^{\infty} \mathrm{Re}\Big[\{-\gamma_0[p(\tau)], p(\tau), \mu_0\}\Big] \\ &\times \tilde{\Omega}_E[p(\tau), t - \tau](\tau^2 - T_R^2)^{-1/2}\mathrm{d}\tau \text{ in } \mathcal{D}_0 \backslash (x_3 = h) \quad (19)\end{aligned}$$

where

$$\tilde{\Omega}_E(p,t) = (1+\tilde{R}_{E0})\tilde{\alpha}_E \exp[-(\tilde{\alpha}_E+\nu_C)t]\mathrm{H}(t) \tag{20}$$

$$\tilde{R}_{E0} = \lim_{s\to\infty} \tilde{R}_E = (\tilde{G}_{E0}-\tilde{G}_{E1})/(\tilde{G}_{E0}+\tilde{G}_{E1}) \tag{21}$$

$$\tilde{\alpha}_E = \beta/(\gamma_0/\mu_0+\gamma_1/\mu_0) \tag{22}$$

and

$$\begin{aligned}\{H_1,H_3,E_2\} &= -\partial_t i(t) * (1/2\pi)\\ &\times \mathrm{Im}\big[\{\gamma_1[p(t)],p(t),\mu_0\}\tilde{\Pi}_E(p)\big]\mathrm{H}(t-T_T)\\ &+\partial_t i(t) * \frac{1}{2\pi}\int_{\tau=T_T}^{\infty}\mathrm{Im}\big[\{\gamma_1[p(\tau)],p(\tau),\mu_0\}\\ &\times \tilde{\Gamma}_E[p(\tau),t-\tau]\big]\mathrm{d}\tau \text{ in } \mathcal{D}_1\end{aligned} \tag{23}$$

where

$$\tilde{\Gamma}_E(p,t) = \tilde{\Pi}_E\tilde{\alpha}_E \exp[-(\tilde{\alpha}_E+\nu_C)t]\mathrm{H}(t) \tag{24}$$

$$\tilde{\Pi}_E = \tilde{T}_{E0}(p)(\partial p/\partial\tau)/\gamma_0(p) \tag{25}$$

$$\tilde{T}_{E0} = \lim_{s\to\infty}\tilde{T}_E = 2\tilde{G}_{E0}/(\tilde{G}_{E0}+\tilde{G}_{E1}) \tag{26}$$

B. TM polarization

The space-time expressions for the TM-polarized fields read the following form

$$\begin{aligned}\{E_1,E_3,H_2\} &= -\partial_t k(t) * \left\{\frac{(x_3-h)t}{D_I^2}, -\frac{x_1 t}{D_I^2}, \epsilon_0\right\}\\ &\times (1/2\pi)(t^2-T_I^2)^{-1/2}\mathrm{H}(t-T_I)\\ &-\partial_t k(t) * \mathrm{Re}\Big[\{\gamma_0[p(t)],-p(t),\epsilon_0\}\tilde{R}_{H0}[p(t)]\Big]\\ &\times (1/2\pi)(t^2-T_R^2)^{-1/2}\mathrm{H}(t-T_R)\\ &-\partial_t k(t) * \frac{1}{2\pi}\int_{\tau=T_R}^{\infty}\mathrm{Re}\Big[\{\gamma_0[p(\tau)],-p(\tau),\epsilon_0\}\Big]\\ &\times \tilde{\Omega}_H[p(\tau),t-\tau](\tau^2-T_R^2)^{-1/2}\mathrm{d}\tau \text{ in } \mathcal{D}_0\backslash(x_3=h)\end{aligned} \tag{27}$$

where

$$\tilde{\Omega}_H(p,t) = (1-\tilde{R}_{H0})\tilde{\alpha}_H \exp[-(\tilde{\alpha}_H+\nu_C)t]\mathrm{H}(t) \tag{28}$$

$$\tilde{R}_{H0} = \lim_{s\to\infty}\tilde{R}_H = (\tilde{G}_{H1}-\tilde{G}_{H0})/(\tilde{G}_{H1}+\tilde{G}_{H0}) \tag{29}$$

$$\tilde{\alpha}_H = \beta/(\epsilon_0/\gamma_0+\epsilon_1/\gamma_1) \tag{30}$$

and

$$\begin{aligned}\{E_1,E_3,H_2\} &= \partial_t k(t) * (1/2\pi)\\ &\times \mathrm{Im}\Big[\Big\{\frac{\epsilon_0}{\epsilon_1}\gamma_1[p(t)], \frac{\epsilon_0}{\epsilon_1}p(t), -\epsilon_0\Big\}\tilde{\Pi}_H(p)\Big]\mathrm{H}(t-T_T)\\ &-\partial_t k(t) * \frac{1}{2\pi}\int_{\tau=T_T}^{\infty}\mathrm{Im}\Big[\Big\{\frac{\epsilon_0}{\epsilon_1}\gamma_1[p(\tau)], \frac{\epsilon_0}{\epsilon_1}p(\tau), -\epsilon_0\Big\}\\ &\times \tilde{\Gamma}_H[p(\tau),t-\tau]\Big]\mathrm{d}\tau \text{ in } \mathcal{D}_1\end{aligned} \tag{31}$$

where

$$\tilde{\Gamma}_H(p,t) = \tilde{\Pi}_H\tilde{\alpha}_H \exp[-(\tilde{\alpha}_H+\nu_C)t]\mathrm{H}(t) \tag{32}$$

$$\tilde{\Pi}_H = \tilde{T}_{H0}(p)(\partial p/\partial\tau)/\gamma_0(p) \tag{33}$$

$$\tilde{T}_{H0} = \lim_{s\to\infty}\tilde{T}_H = 2\tilde{G}_{H1}/(\tilde{G}_{H1}+\tilde{G}_{H0}) \tag{34}$$

V. Discussion of Results

As far as the transform-domain solution is concerned, the expressions do not show any singularities except for the algebraic branch points at $p=\pm 1/c_{0,1}$ (see Eqs. (8), (9) and (13), (14)). The absence of poles implies that no true surface waves, as the Rayleigh wave [16, Sec. 5.11], for example, are excited. However, as the space-time solution shows (see Eqs. (19), (23) and (27), (31)), resulting pulse shapes are dominantly determined by the exponential factors in Eqs. (20), (24) and (28), (32). In them, the real part of factors $\tilde{\alpha}_{E,H}$ and the collision frequency ν_C cause an exponential decay and the imaginary part of $\tilde{\alpha}_{E,H}$ then causes potential oscillations. Upon noting that

$$\tilde{\alpha}_E(p) \propto [c_0\gamma_0(p)+(\epsilon_1/\epsilon_0)^{1/2}c_1\gamma_1(p)]^{-1} \tag{35}$$

$$\tilde{\alpha}_H(p) \propto [1/c_0\gamma_0(p)+(\epsilon_1/\epsilon_0)^{1/2}/c_1\gamma_1(p)]^{-1} \tag{36}$$

we can predict some properties of found space-time expressions. To this end, Eqs. (35) and (36) are evaluated along the path in the first quadrant of the p-plane that corresponds to the reflected waves (see Fig. 2).

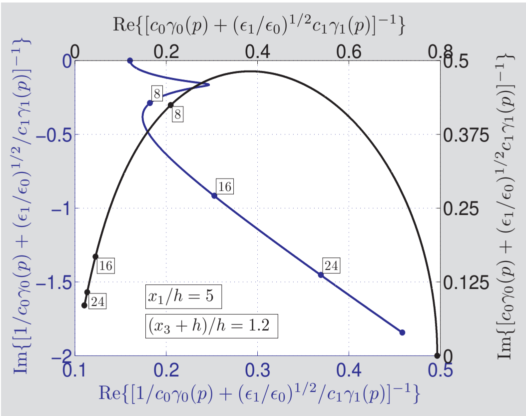

Fig. 2. Trajectories along the Cagniard-DeHoop path evaluated within $T \leq ct/h \leq 30$. The markers along the trajectories are $ct/h = \{8, 16, 24\}$.

Obviously, Eq. (35) approaches zero shortly after the arrival time. As a consequence, no significant surface effects can be expected for the TE-field excitation. On the other hand, the expression connected with the TM fields in Eq. (36) follows a straight line, a slope of which depends on the source/observer offsets x_1 and $Z = x_3 + h$. Its imaginary part predominates over the corresponding real part as the ratio $|x_1|/Z$ increases. Obviously, the ratio is high for large horizontal source/observer offsets and/or if both source and observer are close to the sheet. In this region, a strongly oscillatory effect can be expected provided it is not damped by losses represented by the collision frequency ν_C.

VI. Numerical Results

The space-time expressions given in Sec. IV are evaluated numerically for the TM-polarized field. In our simulations we take the gold sheet of thickness $d = 50$ [nm] and of parameters $\hbar\omega_P = 8.55$ [eV] and $\hbar\nu_C = 0.0184$ [eV] taken from [17]. The

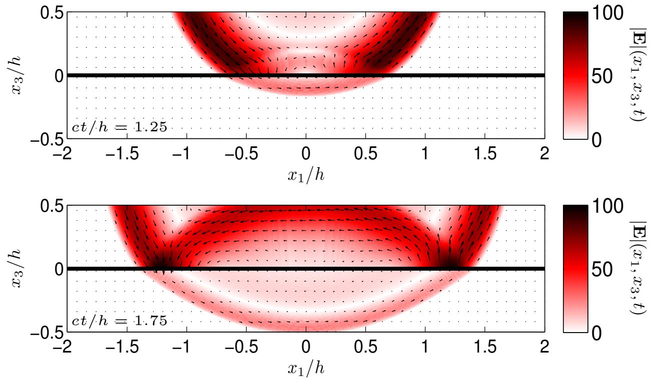

Fig. 3. Time evolution of the electric field strength at $ct/h = \{1.25, 1.75\}$.

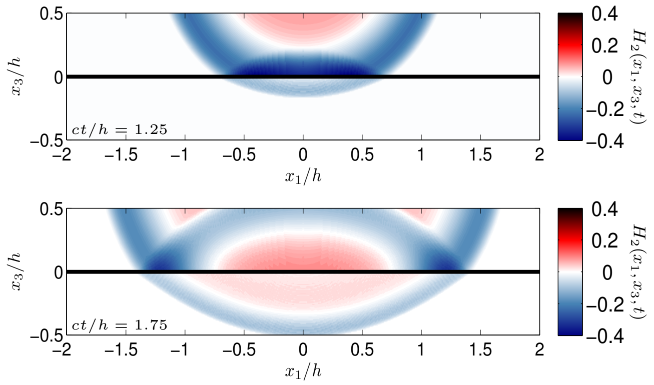

Fig. 4. Time evolution of the magnetic field strength at $ct/h = \{1.25, 1.75\}$.

dielectric support $\mathcal{D}_1$ is described by $\{\epsilon_1, \mu_0\} = \{2.0\epsilon_0, \mu_0\}$, where $\{\epsilon_0, \mu_0\}$ are the constants of vacuum. The TM-polarized field is excited by the magnetic-current line source with the power-exponential source signature

$$k(t) = k_{\rm m}(t/t_{\rm r})^{\nu} \exp[-\nu(t/t_{\rm r} - 1)]\mathrm{H}(t) \tag{37}$$

where we take $k_{\rm m} = 1.0\,[\mathrm{V}]$, $\nu = 2$ and the pulse time width $c_0\, t_{\rm w}/h = 0.5$. The corresponding pulse rise time is $c_0\, t_{\rm r}/h = 0.2707$. Snapshots taken at observation times $ct/h = \{1.25, 1.75\}$ are shown in Figs. 3 and 4. In both figures we can, closely behind the wavefront, observe a significant ridge propagating along the gold surface. This phenomenon becomes stronger as the source moves closer to the interface and its width depends mainly on the pulse time width of the excitation pulse.

VII. Conclusions

Time-domain EM fields excited by line sources placed above thin-film metallic structures have been analysed with the help of the thin-sheet boundary-condition concept and the Cagniard-DeHoop technique. Relaxation effects of analyzed metal films have been accounted for via the Drude model. Closed-form space-time expressions for the pulsed fields have been found and discussed with regard to possible transient excitation of surface plasmon phenomena.

Although no true surface waves can be excited along thin plasmonic metal sheets, it has been shown that for the TM fields, oscillatory surface wave effects can show up. Is is concluded that such phenomena can not be excited for TE polarization. The latter observation is in agreement with the well-known frequency-domain plane-wave solution claiming that surface plasmon polaritons do exist only for TM polarization [7, Sec. 2.2]. However, the time-domain description reveals full extent of complex space-time phenomena that can occur along the surface of a thin metallic sheet. Here in addition to the electromagnetic properties of a metal, the space-time source/observer relationship plays a crucial role.

Acknowledgment

The research described in this paper has been carried out thanks to the financial support of the Operational Programme Education for Competitiveness, project reg. No. CZ.1.07/2.3.00/30.0005, and of the FWO project G.0897.10N. This support is gratefully acknowledged.

References

[1] J. Homola, S. S. Yee, and G. Gauglitz, "Surface plasmon resonance sensors: review," *Sensors Actuat. B*, vol. 54, pp. 3–15, 1999.
[2] K. Kneipp, H. Kneipp, I. Itzkan, R. R. Dasari, and M. S. Feld, "Surface enhanced raman scattering and biophysics," *J. Phys.: Cond. Matt.*, vol. 14, pp. R597–R624, 2002.
[3] H. Ditlbacher, A. Leitner, and F. R. Aussenegg, "Spectrally coded optical data storage by metal nanoparticles," *Opt. Lett.*, vol. 25, pp. 563–565, 2000.
[4] P. Berini, "Plasmon-polariton waves guided by thin lossy metal films of finite width: Bound modes of symmetric structures," *Phys. Rev. B*, vol. 61, p. 1048410503, 2000.
[5] W. L. Barnes, "Surface plasmonpolariton length scales: a route to sub-wavelength optics," *J. Opt. A: Pure Appl. Opt.*, vol. 8, pp. S87–S93, 2006.
[6] J. R. Sambles, G. W. Bradbery, and F. Z. Yang, "Optical-excitation of surface-plasmons – an introduction," *Contemp. Phys.*, vol. 32, pp. 173–183, 1991.
[7] S. A. Maier, *Plasmonics: Fundamentals and applications*. New York, NY: Springer, 2007.
[8] P. B. Allen, "Theory of thermal relaxation of electrons in metals," *Phys. Rev. Lett.*, vol. 59, pp. 1460–1463, 1987.
[9] R. H. M. Groeneveld, R. Sprik, and A. Lagendijk, "Ultrafast relaxation of electrons probed by surface plasmons at a thin silver film," *Phys. Rev. Lett.*, vol. 64, pp. 784–787, 1990.
[10] B. J. Kooij, "Transient electromagnetic field of a vertical magnetic dipole above a plane plasmonic half-space," in *Proc. 2010 URSI EMT Symposium*, Berlin, Germany, Aug. 2010, pp. 181–184.
[11] M. Štumpf and G. A. E. Vandenbosch, "Time-domain behavior of plasmonic half-spaces," *IEEE Photon. J.*, vol. 4, pp. 1236–1246, 2012.
[12] A. T. de Hoop and L. Jiang, "Pulsed em field response of a thin, high-contrast, finely layered structure with dielectric and conductive properties," *IEEE Trans. Antennas Propag.*
[13] A. T. de Hoop, "A modification of Cagniard's method for solving seismic pulse problems," *Applied Scientific Research*, vol. B8, pp. 349–356, 1960.
[14] J. H. M. T. van der Hijden, "Quantitative analysis of the pseudo-Rayleigh phenomenon," *J. Acoust. Soc. Am.*, vol. 75, pp. 1041–1047, 1983.
[15] A. T. de Hoop, *Handbook of radiation and scattering of waves*. London, UK: Academic Press, 1995.
[16] J. D. Achenbach, *Wave propagation in elastic solids*. Amsterdam: North-Holland, 1973.
[17] M. G. Blaber, M. D. Arnold, and M. J. Ford, "Search for the ideal plasmonic nanoshell: The effects of surface scattering and alternatives to gold and silver," *J. Phys. Chem. C.*, vol. 113, pp. 3041–3045, 2009.